DEUTSCHES ELEKTRONEN-SYNCHROTRON DESY

DESY SR-79/09
June 1979

QUANTITATIVE STRUCTURAL STUDIES BY MEANS OF THE ENERGY-DISPERSIVE METHOD WITH X-RAYS FROM A STORAGE RING

by

B. Buras

Physics Laboratory II,
University of Copenhagen
and
Risø National Laboratory, Roskilde

L. Gerward

Laboratory of Applied Physics III,
Technical University of Denmark

A. M. Glazer and M. Hidaka

Clarendon Laboratory, Oxford, U.K.

J. Staun Olsen

Physics Laboratory II. University of Copenhagen

NOTKESTRASSE 85 · 2 HAMBURG 52

To be sure that your preprints are promptly included in the
HIGH ENERGY PHYSICS INDEX ,
send them to the following address (if possible by air mail) :

DESY
Bibliothek
Notkestrasse 85
2 Hamburg 52
Germany

QUANTITATIVE STRUCTURAL STUDIES BY MEANS OF THE ENERGY-DISPERSIVE METHOD WITH X-RAYS FROM A STORAGE RING +

B. BURAS[a,d], L. GERWARD[b], A.M. GLAZER[c], M. HIDAKA[c]

and J. STAUN OLSEN[a]

(a) Physics Laboratory II, University of Copenhagen, Universitetsparken 5, DK-2100 Copenhagen, Denmark.

(b) Laboratory of Applied Physics III, Technical University of Denmark, DK-2800 Lyngby, Denmark.

(c) Clarendon Laboratory, Parks Road, Oxford OX1 3PU, U.K.

(d) Risø National Laboratory, DK-4000 Roskilde, Denmark.

Abstract

Test experiments were made using the X-ray energy-dispersive method at the storage ring DORIS (Hamburg) working in the single-bunch mode. It is shown that the spectral distribution of the incident beam calculated from the storage-ring parameters is in very good agreement with that derived from measured diffraction patterns of known substances, and thus it can be used for structural studies. This is illustrated with results of profile-fitting refinement applied to urea and naphthalene. It is also shown that because of an improved detector system and the time structure of the radiation emitted from the storage ring one is able to record $7 \cdot 10^4$ photons per second and obtain reliable patterns in times of the order of 1 s.

+ Accepted for publication in the Journal of Applied Crystallography

1. Introduction

Structure determination by means of X-ray energy-dispersive diffractometry requires, among other quantities, a knowledge of the spectral distribution and polarization of the radiation incident on the sample. In the case of X-rays from a synchrotron the polarization is well known but beam instabilities occur, particularly during particle extractions. The incident spectrum can be measured using a standard sample with known structural parameters (see e.g. Uno & Ishigaki (1975) or Buras, Staun Olsen, Gerward, Selsmark & Lindegaard-Andersen (1975)). The accuracy of this method is usually worse than with a conventional source (Buras, Staun Olsen, Gerward, Will and Hinze (1977)), although with a dedicated run (i.e. when there is no particle extraction) it has been shown (Bordas, Glazer, Howard and Bourdillon (1977)) that good results can be achieved. An alternative approach is to use a standard sample, approximate the incident spectrum by a polynomial in energy (Glazer, Hidaka and Bordas (1978)) and use the powder-profile fitting method (Rietveld (1969)). However, the need for such a calibration measurement is a nuisance and involves several fitting parameters which may make the method less reliable.

In the present paper we show that the use of synchrotron radiation from a storage ring (in this work DORIS at Hamburg) removes the above-mentioned

difficulties. Our measurements show that the spectral distribution of the incident beam calculated from the machine parameters is in very good agreement with the spectrum derived from the measured diffraction patterns from a known substance, and thus the calculated spectral distribution of the incident beam can be used for structural studies. It is also shown that the stability of the incident spectrum enables reproducible measurements to be made, while the slow decrease of intensity in the course of measurements - a characteristic feature of a storage ring - affects only the statistics, and has no influence on the relative values of the integrated intensities. This is because in energy-dispersive diffractometry all peaks are recorded simultaneously. Thus no monitor is necessary.

An important detector problem in energy-dispersive diffractometry arises when the intensity to be recorded is very high and incompatible with the recording speed of the detector. This problem is discussed in Section 2 of the present paper. It is also shown how some modifications of a system based on a pure germanium detector together with the time-structure of the incident beam can help to increase the maximum count rate.

Section 3 gives examples of quantitative structural analysis using integrated intensities as well as profile-fitting refinement.

2. Experimental Details and Detector Performance

The experimental arrangement at the storage ring is shown in Fig. 1. The slits shown in Fig. 1 define the incident and scattered beams and together with the sample the scattering angle, $2\theta_0$. An ultra-pure germanium detector (Manufacturer: Princeton Gamma-Tech) with pulsed optical feedback was used. The energy analysis of the scattered X-rays was performed using a multichannel pulse-height analyser. We found it convenient to adjust the position of the diffractometer relative to the incident beam and the orientation of the sample by remote control. To simulate typical sample volumes in high-pressure diamond cells the powder samples were placed in Lindemann glass capillaries (0.3 mm internal diameter). For larger samples a Soller slit should be placed in front of the detector.

The storage ring was running in single-bunch mode during our experiments. For DORIS this meant that the radiation emitted by the circulating electrons consisted of pulses approximately every 1 μs with a pulse width of 0.14 ns.

The total dead-time of the detector system, including the multichannel analyser, is 10-15 μs. This means that only one scattered photon can be recorded for each electron bunch and that after each recorded photon 10-15 bunches pass by without being detected. In this situation the single-bunch

mode is as good as the multi-bunch mode, providing that the probability of recording one photon from a bunch is not smaller than 1.

Some modifications were made on the optical feedback system of the ultra-pure germanium detector in order to increase its maximum count rate. The manufacturer changed the feedback capacitor from 0.1 to 1 pF. The reset pulse and the inhibitor pulse were made shorter. In addition, the differentiation/integration time of the amplifier was decreased to 2 μs. The modifications described above gave a slight increase of the recorded peak widths: the full width at half maximum (FWHM) increased from 145 eV to 200 eV at 5.9 keV.

The maximum count rate observed in our experiments at DORIS was about 70000 counts in 1 s in live time mode. Fig. 2 shows a spectrum for $BaTiO_3$ obtained at this count rate. Comparison with previous experiments at the synchrotron DESY (Buras et al., 1977) shows that the maximum count rate obtained at DORIS has increased by a factor of ten. This increase is due partly to the above-mentioned modification in the electronics, and partly to the time-structure of the radiation from the storage ring, so different from that from a synchrotron.

To give some idea of the effect of exposure time on the quantitative analysis of the intensities we show in Table 1 some results for $BaTiO_3$ powder

using data collected over 100, 10 and 1 sec in live time mode. The peak profiles were refined, as described in section 3.2, with the structural parameters fixed at the literature values.

It is seen that even for data collected in 1 sec the reliability factors (defined in 3.2) are quite acceptable and can be considered to be sufficiently good in many cases where high-precision structure analysis is not the primary aim. An analysis of data from silicon shows that a pattern obtained in 100 ms, under the present conditions of DORIS, enables interplanar spacings to be determined with a precision of 0.2-0.4%.

3. Quantitative Structure Analysis from Diffracted Intensities

3.1 Use of integrated intensities

The integrated intensity of a diffraction peak is calculated (after background subtraction) either by summation of the counts in each channel or by fitting the peak to a Gaussian profile and calculating the area under the peak. The theoretical formula for the integrated intensity, I_H, recorded by the detector is given by (Buras and Gerward, 1975; Buras et al., 1977)

$$I_H = C\, i_0(E)\, E^{-2}\, p_H |F_H^2|\, \eta(E)\, A_s(E,\theta_0) A_{air}(E)\, A_{Be}(E)/\sin^3\theta_0 \qquad (1)$$

where C is a constant, E is the energy at the peak maximum, $i_0(E)$ the photon flux in vacuo per unit area and per unit interval of energy, $\eta(E)$ the detector efficiency, $A_s(E,\theta_0)$ the absorption factor of the sample, $A_{air}(E)$ the absorption factor due to the beam path in air and $A_{Be}(E)$ the absorption factor of the beryllium window at the end of the evacuated beam pipe (see Fig. 1), p_H the multiplicity factor, and F_H the structure factor. The spectral distribution of the radiation emitted in vacuum by the relativistic electrons can be calculated using the formulae of Schwinger (1946, 1949).

An alternative way of calculating $i_0(E)$ is to use equation (1) and insert the observed integrated intensities from a sample with known structure factors. This will give $i_0(E)$ at certain discrete points as shown in Fig. 3.

Here, the experimental points were calculated from the integrated intensities of a silicon powder specimen. Absorption coefficients were taken from the International Tables of X-ray Crystallography, Vol. IV (1974) and fitted to a suitable power curve as a function of energy. The absorption factor of the cylindrical sample was calculated using the computer program of Dwiggins (1975). The full line in Fig. 3 was calculated from the machine parameters of DORIS. It is seen that the spectral distribution of the photon flux in vacuo is very close to a straight line on a semilogarithmic diagram i.e. it can be approximated by

$$i_0(E) = a \exp(-bE) \qquad (2)$$

where a and b are constants for a given electron energy. A similar relationship has also been observed by Bathow, Freytag and Haensel (1966) for the radiation from the synchrotron DESY.

The photon-flux density in Fig. 3 is given in arbitrary units. Thus the constant a in equation (2) is used as a scaling factor. However, the slope of the line on the semilogarithmic diagram is given in absolute units. The calculations using the machine parameters of DORIS give $b = 0.1131\ \mathrm{keV}^{-1}$. A least-squares fit to the silicon experimental points gives $b = 0.1118\ \mathrm{keV}^{-1}$,

and therefore the agreement is to within about 1%.

Table 2 shows an example of the determination of the structure factors of iron, using integrated intensities with $i_0(E) = a \exp(-0.1131\ E\ (keV))$. It is seen that the structure factors can be determined with an R-factor of about 3% in this way.

When applying the absorption correction for a powdered sample one has to know the ratio between the density of the powder and that of the solid material. We have used this ratio as a fitting parameter, which has been refined to give the best fit between experimental and theoretical structure factors. The values used are in the range 0.5 to 0.6. For a solid sample or a liquid this complication does not exist and all factors in equation (1), except the constant C, are calculable without refinement.

The results above show with confidence that it is possible to calculate the intensity of the incident beam directly from the known characteristics of the storage ring, taking into account the appropriate absorption corrections. This was not possible with data collected on synchrotrons, such as DESY or NINA, because of inherent beam instabilities, particularly during particle extraction.

3.2 Profile-fitting refinement

The method of profile-fitting refinement applied to energy-dispersive

X-ray diffractometry has been described by Glazer et al. (1978). In that work the intensity of the incident beam was included into an instrument function together with the absorption factors and the detector efficiency. The instrument function was then assumed to be given by a polynomial in energy and included in the refinement procedure. The main advantage of profile-fitting refinement is that it allows quite complicated powder patterns (where there are overlapping reflections) to be analysed.

In the present work the energy-dependence of the incident photon flux in vacuo is known, as discussed in the preceding section. The analytical approximation in equation (2) has been used. The absorption in the sample has then been taken into account by an effective thickness parameter, t, included in the refinement procedure.

The observed profile is fitted to the following expression*)

$$Y_{iH} = C\ i_0(E_i+Z)\cdot[E_i+Z]^{-2}\cdot p_H|F_H|^2\cdot A(E_i+Z)\sin^{-3}\theta_0\cdot W_{iH} \qquad (3)$$

*) The formulae used in this paper are equivalent to the ones used by Glazer et al. (1978), although they are slightly modified and therefore look a little different. This modification means that the instrument function (the energy-dependent correction, excepting that due to the sample) used by Glazer et al. has a different form, since there, Y_{iH} depended on $(E_i+Z)^{-1}$ whereas here it depends on $(E_i+Z)^{-2}$, which is consistent with formula (1) used in this paper.

where Y_{iH} is the number of counts in the i^{th} channel of the pulse-height analyser, C a scale factor, Z zero error and A absorption factor. The probability that photons are diffracted into the i^{th} channel, W_{iH}, is assumed to be given by a Gaussian distribution:

$$W_{iH} = \left(\frac{\ell n 2}{\pi}\right)^{\frac{1}{2}} (2/D_H) \exp\left[-4\ \ell n 2 (E_H - E_{iH})^2 / D_H^2\right] \cdot \Delta E_i \qquad (4)$$

where D_H is the full width at half maximum of the diffraction peak with indices hkℓ, E_H the energy at peak maximum and ΔE_i the energy range per channel. It is also assumed that D_H is a linear function of energy, i.e.

$$D_H = U\ E_H + V\ , \qquad (5)$$

where U and V are fitting parameters.

To illustrate the profile-fitting refinement two examples, urea (NH_2-CO-NH_2) and naphthalene ($C_{10}H_8$) will be described.

Fig. 4 shows the primary diffraction pattern of urea as obtained at DORIS. After subtracting the background, using linear interpolation below the peaks, refinement was carried out for the structural parameters and U, V, and Z, the quantity $i_0(E_i+Z)$ being fixed by equation (2). The effective thickness, t, was also included in the refinement. Because of high correlation between the C and O coordinates it was found necessary to constrain the C-O

bond to remain of fixed length. This is shown in Table 3 together with the results of the refinement procedure. The angle θ_0 was adjusted slightly to obtain the best fit, as it was found that the reliability factors depended very sensitively on this angle. Fig. 5 shows the observed and calculated profiles.

The reliability factors are defined as follows:

(a) for the fitted profile

$$R_{prof} = \sum_i |Y_i(obs) - Y_i(calc)| / \sum_i Y_i(obs)$$

(b) for the integrated intensities

$$R_{int} = \sum_H |I_H(obs) - I_H(calc)| / \sum_H I_H(obs).$$

It is seen that R_{prof} is 10% and R_{int} around 5%, both acceptably low. The sensitivity of the method is demonstrated by the fact that it was necessary to include the scattering contributions of the hydrogen atoms in the calculations in order for the nitrogen coordinates to refine to the correct values. The agreement between these results and the literature values is excellent.

Naphthalene represents a more serious challenge to the method, as it is a more complicated molecule with all atoms on general positions and it is of low symmetry. Accordingly there are many overlapping reflections and so

it is interesting to see what a rather low-resolution technique such as this can achieve. With the atoms all on general positions there are many structural parameters to refine, and so in order to make the problem tractable a rigid-body constraint (Pawley, 1969) was applied. In this, the molecular shape was fixed and refinement was carried out for three Euler angles ψ, θ and ϕ (defining the molecular orientation) and overall temperature factor. Table 4 gives the reults and Fig. 6 shows the observed and calculated profiles. The rapid convergence and low standard deviations of the Euler angles indicate that the refinement is good and this is supported by the reasonable values for the reliability factors*). Comparison of the atomic coordinates thus obtained with those of Cruickshank (1957) shows a very close agreement for all atoms, thus giving confidence in the method. This represents the most complicated structure yet analysed with the energy-dispersive technique.

---

*) The reliability factor for the fitted profile equal to 0.14 has a similar value as those obtained for structures of similar complication using the monochromatic neutron beam diffraction technique and the rigid-body constraint (see e.g. Mackenzie, Buras & Pawley (1978) and references therein).

Acknowledgements

We should like to express our thanks to DESY, in particular to Prof. G. Weber, Research Director, for permission to perform the test and to Prof. C. Kunz, Dr. E.E. Koch and Dr. G. Materlik for their interest and help during the course of this work. We should also like to thank Prof. A. Lindegaard-Andersen for helpful discussions. The substantial technical help of Mr. F. Ferrall is greatly appreciated. We are grateful too to the Director and staff of the Daresbury Laboratory for computing facilities.

The work reported here was made possible by grants from the Danish Natural Sciences Research Council and the Science Research Council (U.K.). This financial support is gratefully acknowledged.

References

BATHOW, G., FREYTAG, E. and HAENSEL, R. (1966) J. Appl. Phys. 37, 3449-3454.

BORDAS, J., GLAZER, A.M., HOWARD, C.J. and BOURDILLON, A.J. (1977)
Phil. Mag. 35, 311-323.

BURAS, B., STAUN OLSEN, J., GERWARD, L., SELSMARK, B. and LINDEGAARD-ANDERSEN, A.
(1975) Acta Cryst. A31, 327-333.

BURAS, B. and GERWARD, L. (1975) Acta Cryst. A31, 372-374.

BURAS, B., STAUN OLSEN, J., GERWARD, L., WILL, G. and HINZE, E. (1977).
J. Appl. Cryst. 10, 431-438.

CRUICKSHANK, D.W.J. (1957) Acta Cryst. 10, 504-508.

DWIGGINS, C.W. Jr. (1975) Acta Cryst. A31, 146-148.

GLAZER, A.M., HIDAKA, M. and BORDAS, J. (1978) J. Appl. Cryst. 11, 165-172.

International Tables for X-ray Crystallography, Vol. IV, Kynoch Press,
Birmingham 1974.

MACKENZIE, G.A., BURAS, B, and PAWLEY, G.S. (1978) Acta Cryst. B34, 1918-1923.

PAWLEY, G.S. (1969) Acta Cryst. A25, 531-535.

RIETVELD, H.M. (1969) J. Appl. Cryst. 2, 65-71.

SCHWINGER, J. (1946) Phys. Rev. 70, 798-799; (1949) Phys. Rev. 75, 1912-1925.

UNO, R. and ISHIGAKI, A. (1975) J. Appl. Cryst. 8, 578-581.

VAUGHAN, P. and DONOHUE, J. (1952) Acta Cryst. 5, 530-535.

Table 1

Dependence of the reliability factors on exposure time

$BaTiO_3$ powder, $2\theta_0 = 16.441^\circ$ (refined parameter)

		Exposure time (sec)		
		100	10	1
	R_{prof}	0.060	0.11	0.16
	R_{int}	0.043	0.055	0.073
Refined parameters	C	2.01(4)	0.199(7)	0.020(1)
	U	0.0058(10)	0.0053(17)	0.0066(26)
	V (keV)	0.22(2)	0.22(4)	0.19(6)
	Z (keV)	0.025(1)	-0.057(2)	-0.056(3)
	t (cm)	0.0118(2)	0.0121(3)	0.0121(5)

The various reliability factors are defined in section 3.2.

Table 2

Structure factors for iron calculated from integrated intensities. The intensity of the primary beam has been calculated from the machine parameters of DORIS.

hkℓ	$\|F_{exp}\|$	$\|F_{theor}\|$	$\|\Delta F\|$
220	20.2	21.4	1.2
310	19.1	19.0	0.1
222	17.5	17.1	0.4
321	16.2	15.6	0.6
400	14.7	14.5	0.2
411/330	14.0	13.5	0.5
420	13.1	12.7	0.4
332	12.4	12.0	0.4
422	11.7	11.3	0.4
510/413	10.6	10.8	0.2
521	10.2	9.9	0.3
440	9.4	9.5	0.1
530/433	9.2	9.1	0.1
600/442	8.6	8.7	0.1
611/532	8.6	8.4	0.2
620	7.6	8.1	0.5
541	7.9	7.8	0.1
622	6.6	7.5	0.9
631	6.9	7.2	0.3
710/550/543	6.9	6.7	0.2
721/633/552	6.3	6.3	0.0
642	5.4	6.0	0.6

$R = \sum|\Delta F| / \sum|F| = 0.032$

Table 3

Results of profile-fitting refinement

Urea (NH_2-CO-NH_2)$P\bar{4}2_1n$ a = b = 5.661 Å, c = 4.712 Å.

Constraints:

Atom	Parameter
O	x = 0, y = ½,
C	x = 0, y = ½, z(O) = z(C) + 0.268
N	y = x + ½
H	x = 0.253, y = x + ½, z = 0.287
	x = 0.137, y = x + ½, z = 0.972

Refined profile parameters:

C	U	V(keV)	Z(keV)	t(cm)
4.05(6)	0.009(1)	0.16(2)	-0.023(1)	0.028(6)

Refined fitting parameters

Atom	Parameter	Refined value	Vaughan and Donohue (1952)
O	z	0.5939(19)	0.5987
	B (Å^2)	3.2(3)	
N	x	0.1455(8)	0.1429
	z	0.1851(21)	0.1848
	B (Å^2)	3.3(3)	
$2\theta_0$ = 16.334°, refined parameter			
R_{prof} = 0.10, R_{int} = 0.054			

Table 4

Results of profile-fitting refinement

Naphthalene ($C_{10}H_8$) $P2_1/a$

a = 8.235 Å, b = 6.003 Å, c = 8.658 Å. β = 122° 55'

Refined profile parameters:

C	U	V (keV)	Z (keV)	t (cm)
2.61(7)	0.008(2)	0.17(4)	0.074(2)	0.005

Refined Euler angles and overall temperature factor:

ψ (°)	θ (°)	φ (°)	B (Å^2)
-62.116(4)	-71.960(3)	67.511(7)	5.0(5)

Fractional coordinates of atoms:

	refined values			Cruickshank (1957)		
	x	y	z	x	y	z
C(1)	0.0884	0.0209	0.3264	0.0856	0.0186	0.3251
C(2)	0.1164	0.1618	0.2195	0.1148	0.1588	0.2200
C(3)	0.0480	0.1021	0.0352	0.0472	0.1025	0.0351
C(4)	0.0753	0.2458	-0.0701	0.0749	0.2471	-0.0784
C(5)	0.0084	0.1848	-0.2556	0.0116	0.1869	-0.2541
H(1)	0.1402	0.0654	0.4669	0.1375	0.0657	0.4663
H(2)	0.1909	0.3201	0.2741	0.1888	0.3176	0.2752
H(3)	0.1498	0.4042	-0.0246	0.1490	0.4056	-0.0233
H(4)	0.0299	0.2961	-0.3424	0.0345	0.2999	-0.3394
$2\theta_0$ = 16.330°, refined parameter						
R_{prof} = 0.14, R_{int} = 0.061						

Figure Captions

Fig. 1. Experimental arrangement at the storage ring.

Fig. 2. Diffraction spectrum of $BaTiO_3$ (3.7 GeV, 14 mA, $2\theta_0 \approx 16.4^\circ$) as obtained at the storage ring. Exposure time 1 s, e = escape peaks, 42.3 eV/channel.

Fig. 3. Spectral distribution of the photon flux density in vacuo from DORIS for the electron energy 3.7 GeV. The experimental points are calculated from the integrated intensities of a silicon powder. The full line is calculated from the machine parameters of DORIS and is fitted to the experimental points using a single scaling factor (a in eq. (2)).

Fig. 4. Diffraction pattern of urea (3.7 GeV, 12 mA, $2\theta_0 \approx 16.3^\circ$, exposure time 500 s) as obtained at the storage ring.

Fig. 5. The spectrum of Fig. 4 after profile-fitting refinement. Crosses denote the experimental points and the full line the refined profile. The difference between the experimental and fitted profiles is shown by the lower curve. The positions of the reflections are indicated by the small vertical bars.

Fig. 6. Observed and calculated profiles for naphthalene. Exposure time 1200 s. The first peak at low energy was omitted from the refinement as it occurs close to the absorption-edge of the germanium in the detector.

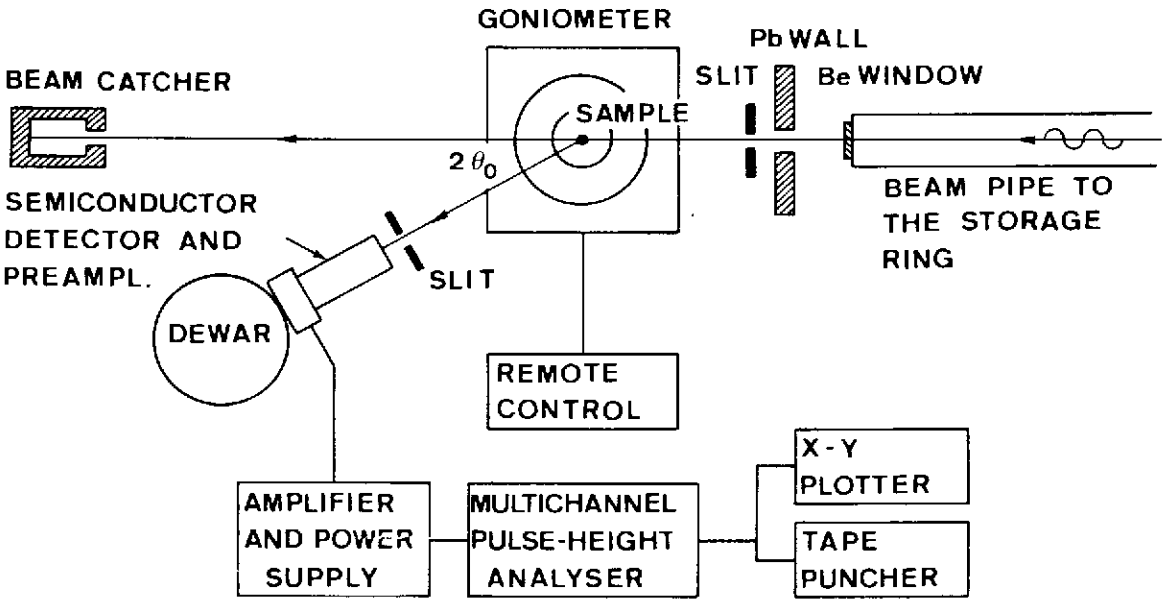

EXPERIMENTAL SET-UP

Fig. 1.

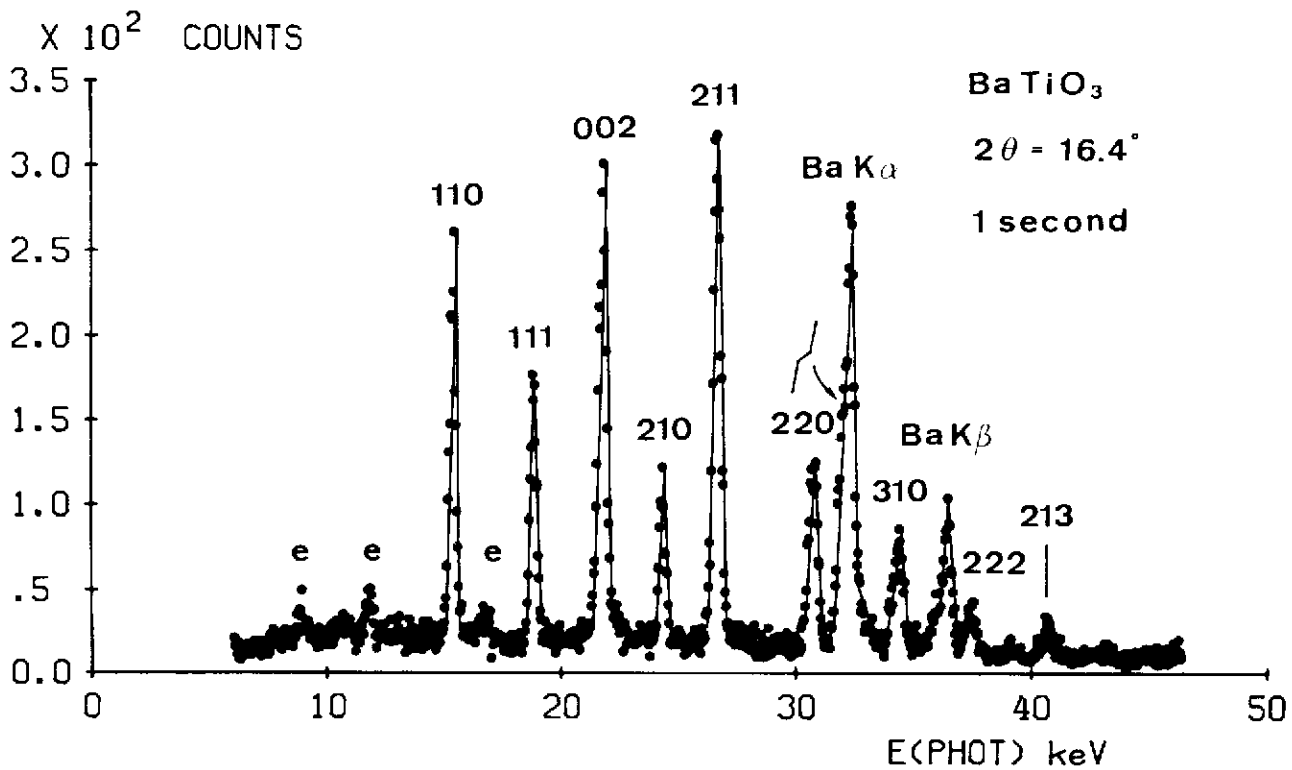

Fig. 2.

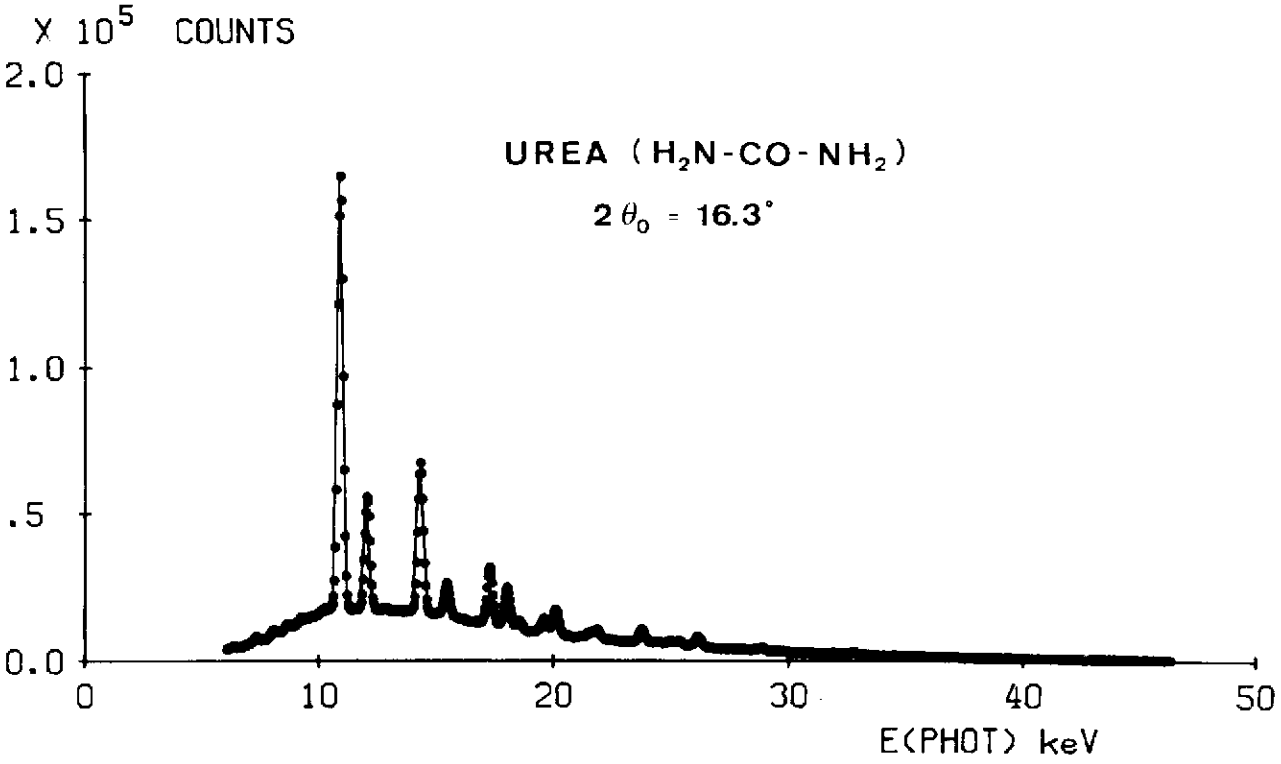
X 10^5 COUNTS
2.0
1.5
1.0
.5
0.0
UREA (H2N-CO-NH2)
2 θ0 = 16.3°
0
10
20
30
40
50
E(PHOT) keV

Fig. 4.

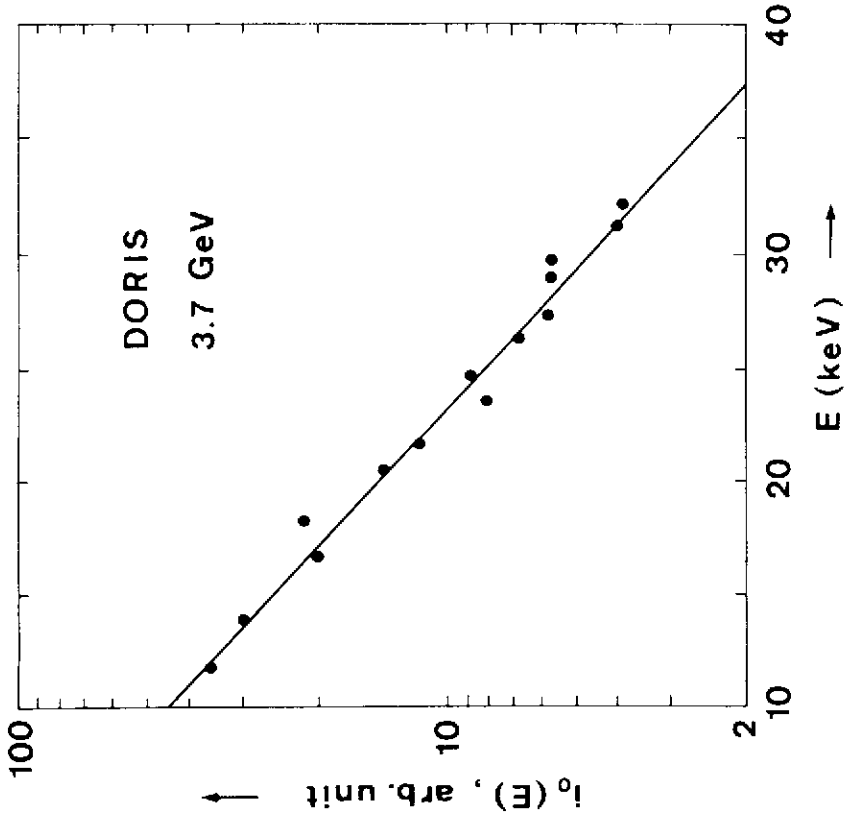
DORIS
3.7 GeV
100
10
2
40
30
20
10
E (keV)
i0 (E) , arb. unit

Fig. 3.

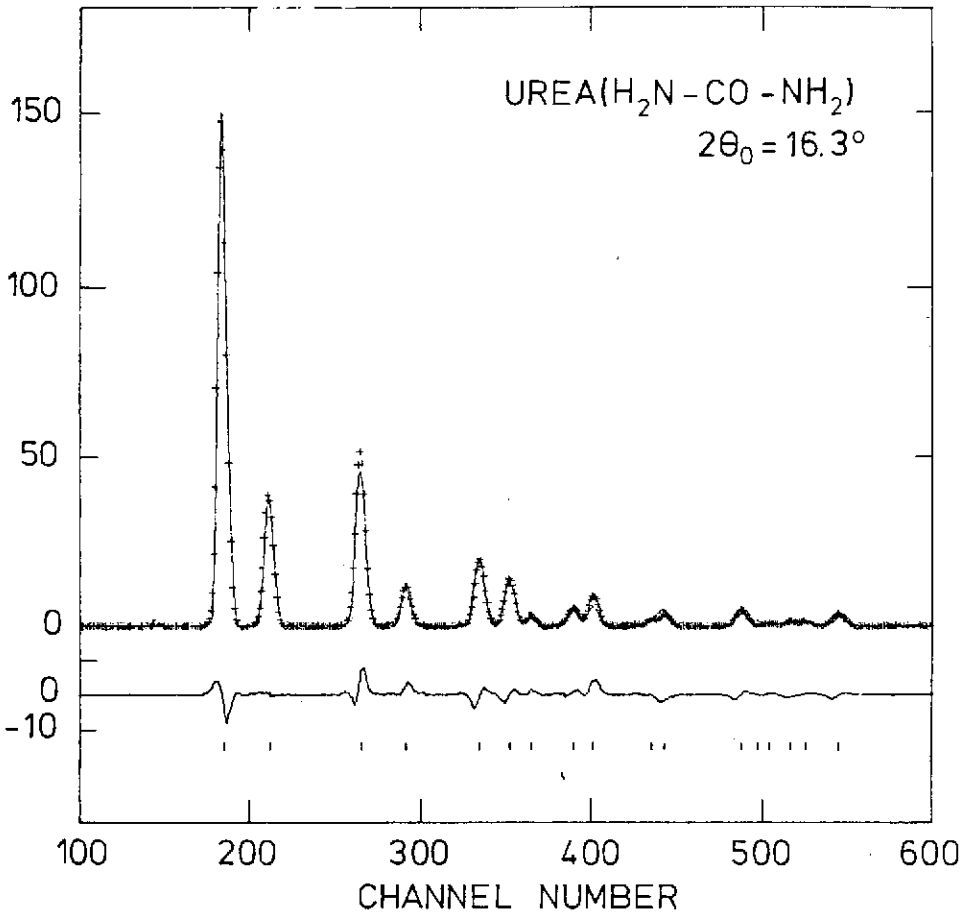
UREA($H_2N-CO-NH_2$)
$2\theta_0 = 16.3°$
150
100
50
0
0
-10
100
200
300
400
500
600
CHANNEL NUMBER

Fig. 5.

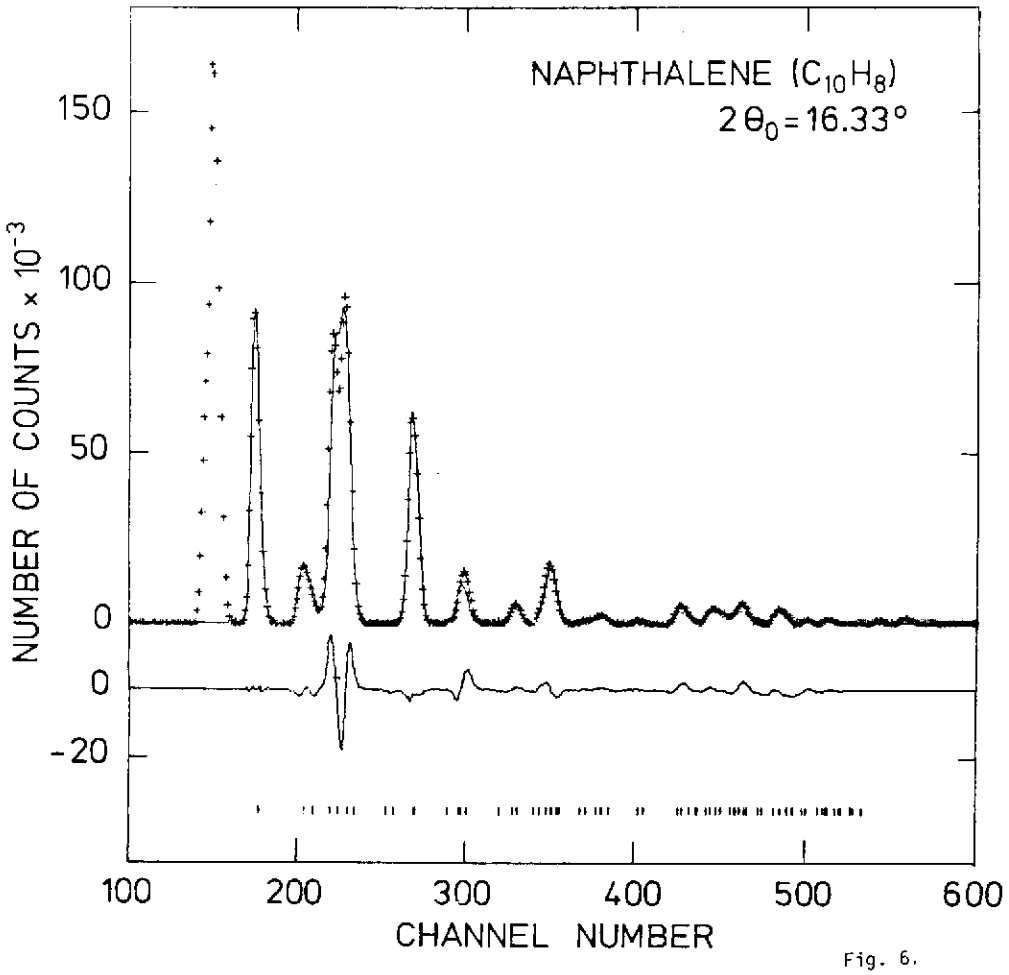
NAPHTHALENE ($C_{10}H_8$)
$2\theta_0 = 16.33°$
NUMBER OF COUNTS × 10^{-3}
150
100
50
0
0
-20
100
200
300
400
500
600
CHANNEL NUMBER

Fig. 6.